

Statistical Properties of Loaded Wireless Multicarrier Systems

Curt Schurgers, *Member, IEEE*, and Mani B. Srivastava, *Senior Member, IEEE*

Abstract—Multicarrier modulation has established itself as an appealing option for high-performance wireless communication systems. When the channel varies slowly in time, such as in applications with low terminal mobility, adaptive loading further enhances the system performance considerably. However, even with adaptive loading, significant performance fluctuations still occur, which impact the higher layers and the overall system behavior. First, a good understanding of the nature of these fluctuations is crucial to design better higher layers that are able to tolerate or combat this variability. For this reason, we develop a full statistical description of a loaded wireless multicarrier system that accurately characterizes its behavior. Our model abstracts the loaded system as an equivalent single carrier system with flat log-normal fading and has the channel tap as a single parameter. Second, with our model, the physical layer can now be incorporated in an abstracted fashion during simulation, resulting in significant speed-ups. Indeed, the alternative would be to include the entire loaded multicarrier system in these simulations, which is highly time consuming. Third, our statistical model is also important for the mathematical analysis of protocols, which requires knowledge of the physical layer statistics. We derive such statistics for both correlated and uncorrelated Rayleigh fading.

Index Terms—Modeling, wireless LAN.

I. INTRODUCTION

PROVIDING broadband wireless services is a challenging task due to the hostile nature of the wireless medium and the limited spectral resources available. A technique that is becoming increasingly popular is wireless multicarrier modulation, which is also known as orthogonal frequency division multiplexing (OFDM) [1]. Unlike traditional single-carrier systems, the used frequency band is subdivided into a large set of narrow subbands, or subcarriers, which are spaced very closely together. Each such subband carries an independent low-rate data stream. Because of the large number of such subbands, the aggregate data rate is high. Besides the resulting high spectral efficiency, its immunity to intersymbol interference is another important benefit of OFDM [1].

Multicarrier modulation has been adopted for digital video broadcast (DVB), digital audio broadcast (DAB), and the wire-

less local area network (WLAN) standards IEEE 802.11a [2] and European Telecommunications Standards Institute (ETSI) HYPERLAN II [20]. Flarion has proposed its variant, called Flash OFDM, for third-generation (3G) systems [22], and CISCO is considering vectored OFDM for digital microwave communications [23]. For these diverse application scenarios, a number of different setups have been suggested. At the multiaccess level, the subcarriers can be divided between users as proposed in [17] and [18]. Alternatively, a single user could transmit in the entire OFDM frequency band, where different users are separated in time through time-division multiple access (TDMA) [2], [3], [20]. At the network level, different cells with the same center frequency can be sufficiently isolated from each other, or otherwise intercell interference has to be taken into account [19]. In this paper, we focus on a system with isolated cells, where multiaccess is handled through TDMA. This setup corresponds to that of WLANs [2], [20], [21]. Adaptive bit loading (also referred to as adaptive loading, bit loading, or loading) can greatly improve the performance of such an OFDM system by leveraging the frequency selective nature of the channel [3], [25]. The idea is to select the constellation size and transmit power on each of the subcarriers depending on their respective signal-to-noise ratio (SNR). Such adaptive loading is not yet included in the current IEEE 802.11a and HYPERLAN II standards but comes as an almost natural extension [21].

Despite the improvements of adaptive loading, channel variations still present themselves to the higher layers as significant fluctuations in the transmission performance, as we will illustrate in this paper. Therefore, these higher layers should be designed specifically to cope with such fluctuations [4]. In order to do this, it is important to clearly understand the behavior of a loaded multicarrier system and the resulting performance. Furthermore, protocol designers use extensive simulations in their evaluation of different alternatives. However, due to the inherent complexity of loaded multicarrier modulation, it is highly time consuming and practically infeasible to simulate it on the bit level together with upper layer protocols. To get meaningful data in an acceptable time frame, a simple model of the loaded system is thus imperative. This model has to exhibit the correct statistical properties. Besides for protocol design, such a model is also needed to derive analytic expressions of protocols working on top of this physical layer.

In related prior work, the average capacity of a multicarrier system has been studied [5]–[7], [26]. Although it provides useful bounds on the performance, it does not constitute a valid model of the loaded OFDM system, as it mostly assumes an infinite number of subcarriers. Even if the actual number of

Manuscript received February 14, 2002; revised October 13, 2004 and November 23, 2004; accepted December 7, 2004. The editor coordinating the review of this paper and approving it for publication is L. Hanzo.

C. Schurgers is with the Electronics and Communications Engineering Department, University of California, San Diego, CA 92093 USA (e-mail: curts@ece.ucsd.edu).

M. B. Srivastava is with the Electrical Engineering Department, University of California, Los Angeles, CA 90095-1476 USA (e-mail: mbs@ee.ucla.edu).

Digital Object Identifier 10.1109/TWC.2005.853822

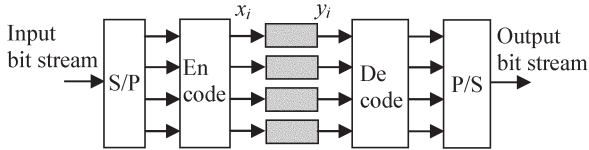


Fig. 1. Conceptual view of a multicarrier system.

subbands is taken into account, only the average capacity is considered [26]. Furthermore, in a real OFDM system, the performance varies over time as the channel changes. This effect is disregarded by considering capacity. A practical model must therefore take into account the bounded number of subcarriers and capture time variations. In this paper, we derive such a model that shows that loaded OFDM essentially offers the look and feel of a single-carrier system. Details of the parallel subcarriers and the loading are hidden inside this model. It nevertheless captures the statistical characteristics of the loaded system and speeds up simulations since no explicit bit loading has to be performed.

II. MULTICARRIER SYSTEM

A. Basic Multicarrier System

A conceptual (rather than implementation-oriented) view of a multicarrier system is presented in Fig. 1. The input bit stream is split up into N parallel streams that are individually mapped to transmit symbols x_i by the encoder. In this notation, i is the subcarrier index. The shaded boxes represent the channels for these N subcarriers. At the receiver, the symbols y_i are decoded and aggregated into one outgoing bit stream.

Typically, each subcarrier is modulated using quadratic amplitude modulation (QAM) [8, pp. 178–181]. When assuming perfect carrier phase estimation and sufficiently fast channel estimation updates, each subcarrier experiences static flat fading [1], [3], [8]. In this case, the performance on the i th subcarrier in terms of bit-error rate (BER) and symbol-error rate (SER) is well approximated by [8, p. 280]

$$\text{BER}_i = \frac{\text{SER}_i}{b_i} = \frac{K_i}{b_i} Q \left(\sqrt{3 \frac{\text{SNR}_i}{2^{b_i} - 1}} \right) \quad (1)$$

$$\text{SNR}_i = \alpha_i \frac{P_i}{P_n} A \quad (2)$$

$$K_i = 4 \left(1 - \frac{1}{2^{\frac{b_i}{2}}} \right). \quad (3)$$

In (1), b_i is the constellation size in bits per symbol. The received SNR on the i th subcarrier is defined as (2), where P_i is the transmit power on that subcarrier. Depending on the spacing between the subcarriers with respect to the channel coherence bandwidth, the channel gain factors α_i are either correlated or uncorrelated. Irrespective of their mutual correlation, they exhibit a Chi-square probability density function (pdf) with two degrees of freedom in the case of Rayleigh fading. This type of fading describes wireless radio communications in the

absence of a line-of-sight path between sender and receiver [8]. The noise power P_n is set constant without loss of generality, as unequal values can be lumped into parameter α_i [8]. Since we do not have an intercell interference in our system setup, this noise is uncorrelated on different subcarriers. Factor A contains the large-scale propagation effects like path loss and shadowing. More generally, the performance can be described by (4) in terms of the gap Γ_i [9]

$$b_i = \log_2 \left(1 + \frac{\text{SNR}_i}{\Gamma_i} \right). \quad (4)$$

This gap Γ_i measures the SNR loss compared to capacity. It is dependent on the SER, the coding scheme, and the system implementation. For uncoded QAM, it can be directly derived from (1) as being equal to

$$\Gamma_i = \frac{\left[Q^{-1} \left(\frac{\text{SER}_i}{K_i} \right) \right]^2}{3}. \quad (5)$$

B. Adaptive Bit-Loading

Bit-loading algorithms assign P_i and b_i to different subcarriers to optimize system performance. Several practical loading algorithms have been published [9]–[15]. A common trait is the fact that the performance is made identical on each of the subcarriers, which is indeed optimal. Strictly speaking, this would mean that the SER_i is the same (or better yet, the BER_i), but in practice SER_i/K_i or equivalently Γ_i is made constant over the subcarriers

$$\Gamma_i = \Gamma \Leftrightarrow \frac{\text{SER}_i}{K_i} = \frac{\text{SER}}{K}. \quad (6)$$

Note that typically some subcarriers are not loaded at all when it is inefficient for them to carry any information [10]–[12]. Those are the ones with the lowest values of α_i , and they end up with P_i and b_i both equal to 0. We define \tilde{N} as the numbers of subcarriers that are loaded and therefore carry information. From now on, we assume that α_i are ordered in descending order, without loss of generality (as this is simply a reindexing operation). It is clear that the first \tilde{N} subcarriers are loaded and the rest remain unloaded. This allows us to simplify our analytical expressions considerably.

III. SINGLE PARAMETER DESCRIPTION

In Appendix A, we derive a compact exact expression for the overall performance of a multicarrier system. We show that the BER as seen by an external observer follows (7)–(8). In this equation, P_{av} is the average transmit power, defined as in (9). Equation (10) gives the average number of bits per subcarrier in an OFDM symbol, called the target loading rate b_{av} , which is an input to the loading algorithm. From a black-box point of view, the system essentially offers the look and feel of a

flat-fading single-carrier QAM system with the same average transmit power and bit rate.

$$\text{BER} = \frac{K}{b_{\text{av}}} Q \left(\sqrt{3 \frac{\delta}{2^{b_{\text{av}}} - 1} \frac{P_{\text{av}}}{P_n} A} \right) \quad (7)$$

$$K = 4 \left(1 - \frac{1}{2^{\frac{b_{\text{av}}}{2}}} \right) \quad (8)$$

$$P_{\text{av}} = \frac{1}{N} \sum_{i=1}^N P_i \quad (9)$$

$$b_{\text{av}} = \frac{1}{N} \sum_{i=1}^N b_i. \quad (10)$$

The crucial parameter in (7) is the flat fading channel tap δ . It depends on the bit-loading assignments b_i and the channel gain factors, as given by (11). This expression is valid independent of the loading algorithm, the constraints on the values of b_i , or the correlation between the subcarriers (see also Appendix A)

$$\delta = \frac{2^{b_{\text{av}}} - 1}{\frac{1}{N} \sum_{i=1}^{\tilde{N}} \frac{2^{b_i} - 1}{\alpha_i}}. \quad (11)$$

For a specific target loading rate, (7) governs the relationship between the transmit power (or equivalently the SNR) and the resulting BER performance. This relationship only depends on one parameter, the fading tap δ , which is independent of the SNR and therefore characterizes the entire BER–SNR curve in just one number. Upon closer investigation of (7), we notice that this equation corresponds to the system model depicted in Fig. 2. The loaded system can thus be represented as a virtual single-carrier QAM system with a flat-fading channel tap. The specifics of the N parallel subcarriers, the bit loading, and the serial-parallel conversion are all hidden inside the parameter δ .

To validate this description, we carried out simulations based on the algorithm proposed in [15], which is a variation of the Hughes–Hartoghs algorithm [10]–[12]. We set $N = 100$ and the target loading rate is specified as $b_{\text{av}} = 4$ bits/symbol. For the simulations of Fig. 3, one channel is created with uncorrelated gain factors picked from a Chi-square distribution. After loading, δ was calculated using (11) and the curve for our model was generated through (7). The curve marked “bit true” is completely based on bit-true simulations of the loaded OFDM system, performing QAM modulation under perfect channel estimation conditions. As a basis of comparison, we show the curve for an unloaded multicarrier system on the same channel together with that for an additive white Gaussian noise (AWGN) channel. In both of these cases, 16-QAM modulation is used, resulting in the same average throughput as the loaded system. We observe that adaptive loading greatly improves the system performance and that its simulated performance corresponds well to our analytic

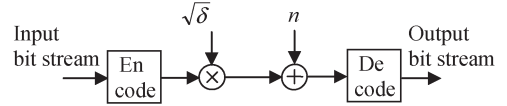


Fig. 2. Model for the loaded multicarrier system.

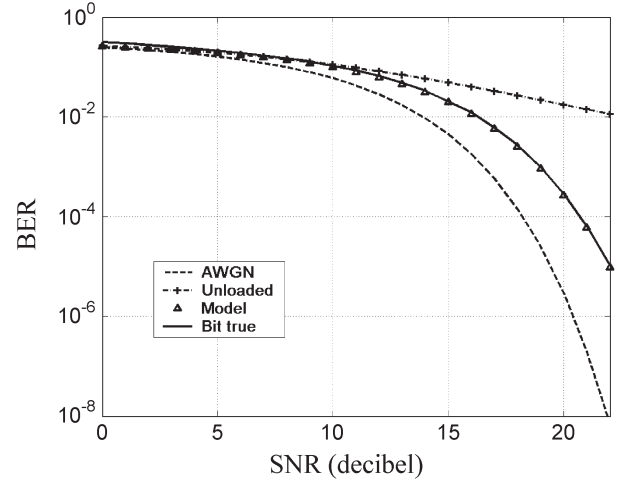


Fig. 3. Comparison of our analytic model to simulations.

description. From (7) and Fig. 3, we also see that for a particular wireless channel there is a fixed power penalty compared to the AWGN channel with the same P_{av} and b_{av} . Adaptive loading therefore in effect “whitens” the channel.

Note that bit-loading algorithms require knowledge of the channel gains. As a result, channel estimation is needed and has to be updated regularly. In order to avoid severe performance penalties, the channel gains have to remain almost constant between two updates. Bit loading therefore makes sense only when the update rate is sufficiently fast compared to the Doppler rate of the channel [21]. After loading, the entire relevant instantaneous state of the physical layer is condensed into a single parameter δ . Since the channel stays virtually constant between updates, this parameter remains valid over this time period as well. Over longer time scales, δ changes as the underlying channel varies according to the Doppler rate.

When simulating systems that have a loaded multicarrier system as a physical layer, we only need to know δ , as we have illustrated in Fig. 3. However, in most cases, it is undesirable to generate this parameter by performing adaptive loading on a detailed channel. Instead, it would be better to generate δ directly as a random variable, leading to a stochastic model. From (11), we observe that δ depends on the specific values of the N channel gains. When we record the value of δ over a long time, or equivalently consider a large number of different channels, we can build a histogram that predicts its pdf. A complete stochastic model also has to include the time variations of the underlying channel, which are characterized by the Doppler rate.

The remaining task to complete our stochastic model is to derive the pdf of δ . In the next section, we assume uncorrelated fading across the subcarriers, where α_i are independent

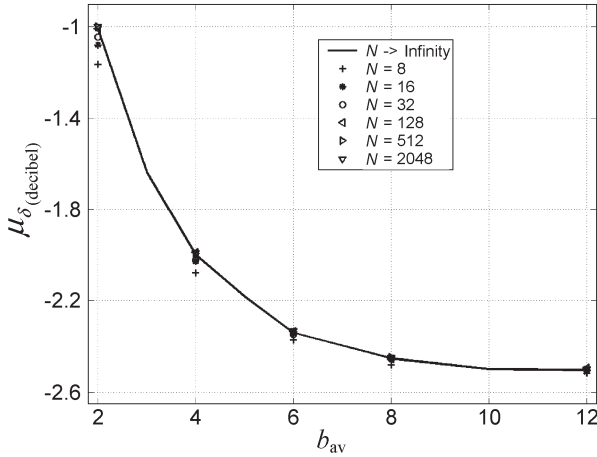


Fig. 4. $\mu_{\delta(\text{decibel})}$ versus b_{av} for water filling and uncorrelated fading.

from one subcarrier to the next and expand the solution to correlated fading in Section V.

IV. PDF OF δ FOR UNCORRELATED FADING

A. Model for Water Filling

For practical bit-loading algorithms, finding the statistics of δ is very hard. We therefore investigate first what the solution looks like for the theoretically optimal assignment and adjust the results for practical algorithms. This theoretical optimum assignment of power and bits over the subcarriers is known as water filling [16] and assumes an infinitesimal granularity in constellation sizes (i.e., fractional values of b_i). Real-life systems can only have constellations with an integer number of points, typically a power of two.

To conserve the flow of this paper, we have moved the derivation of the statistics to Appendix B and summarize the results here. In the case of water filling, δ is approximately log-normally distributed for not too small N . As shown in Appendix B, the reason is that for a sufficiently large value of N , the central limit theorem can be invoked. Simulations, which we will present later on, illustrate this to occur approximately when $N > 32$. The entire distribution can thus be described by the mean and variance of $10 \log_{10}(\delta)$ or, equivalently, of δ expressed in decibels. This mean value is defined by the coupled integral equations

$$b_{av} = \int_{\tilde{\alpha}}^{\infty} \left[\log_2 \left(\frac{1}{\tilde{\alpha}} \right) - \log_2 \left(\frac{1}{\alpha} \right) \right] f_{\alpha}(\alpha) d\alpha \quad (12)$$

$$\frac{2^{b_{av}} - 1}{\delta} = \int_{\tilde{\alpha}}^{\infty} \left[\frac{1}{\tilde{\alpha}} - \frac{1}{\alpha} \right] f_{\alpha}(\alpha) d\alpha \quad (13)$$

where $f_{\alpha}(\alpha)$ represents the pdf of the channel gains. In our analysis, we choose a Chi-square distribution, which corresponds to the case of Rayleigh fading. Although closed-form solutions to these coupled equations are not available for most practical distributions, numerical integration or root-finding techniques can be used to solve this problem [6].

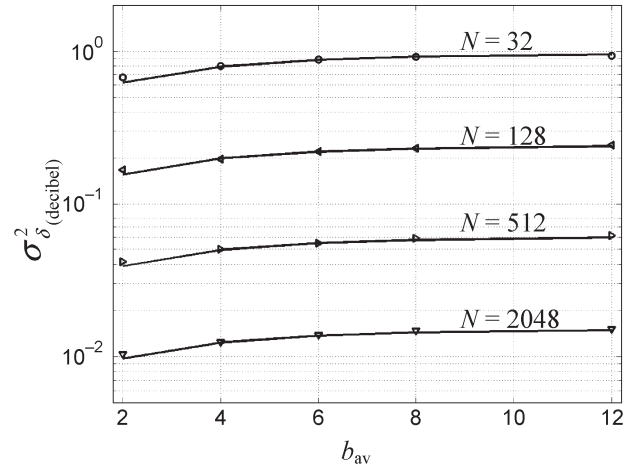


Fig. 5. $\sigma_{\delta(\text{decibel})}^2$ versus b_{av} for water filling and uncorrelated fading.

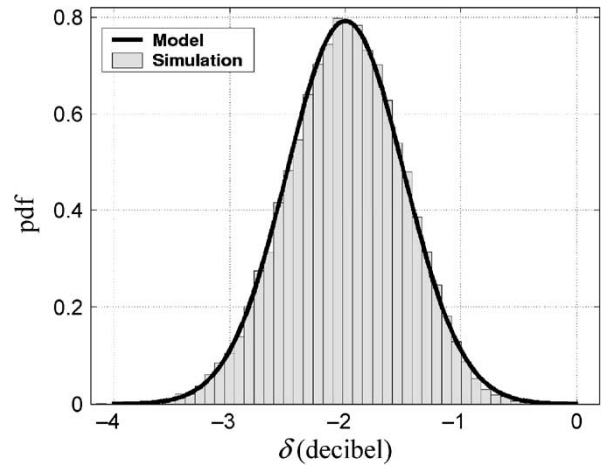


Fig. 6. Simulated results and model for the pdf of δ for water filling and uncorrelated fading.

The variance of δ (in decibels) is expressed as

$$\sigma_{10 \log_{10}(\delta)}^2 = \left(1 - \sqrt{2^{-(1+\theta \cdot b_{av})}} \right) \cdot \frac{\sigma_{10 \log_{10}(\alpha_i)}^2}{N} \quad (14)$$

with $\theta = 1$.

We have verified the above model for water filling through simulations. Fig. 4 plots the mean value of δ (in decibels) versus b_{av} for different N . The curve for $N \rightarrow \infty$ is obtained from (12) and (13), which also corresponds to the results reported in [5] and [6] for average capacity. When $N > 32$, this analytic result is indeed very close to the simulated values. Equation (14) for the variance is depicted as the solid lines in Fig. 5. The markers denote simulated results, which only rely on the definition of variance and do not make any assumption about the underlying distribution. We again observe a tight correspondence between simulations and analytic results. Finally, we validate the complete pdf in Fig. 6, which compares it to the simulated histogram of δ (in decibels) for $N = 100$ and $b_{av} = 4$ bits/symbol. We have conducted many more simulations for a whole range of (N, b_{av}) tuples. All these simulations for $N > 32$ resulted in fits comparable to the one in Fig. 6.

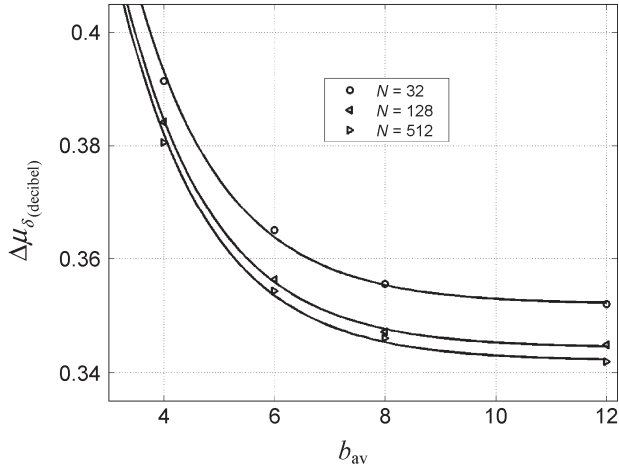


Fig. 7. $\Delta\mu_{\delta(\text{decibel})}$ versus b_{av} for uncorrelated fading.

This log-normal distribution appears to be very good indeed to model the statistics of δ after water filling. However, in deriving our model in Appendix B, some simplifications were made to approximate the true distribution. Although a log-normal distribution appears to be a good practical fit, hypothesis matching such as the Kolmogorov–Smirnov goodness-of-fit test is not appropriate since by design the log-normal distribution is only an approximation of the true statistics [24]. We will illustrate in Section VI that our approximation yields a statistical model that is both easy to use and sufficiently accurate in practice.

B. Model for Loading Algorithms

For practical loading algorithms, a mathematical derivation of the distribution of δ gets extremely involved. Nevertheless, as all these algorithms try to approximate water filling, it is likely that a more or less direct extension of the results of the previous subsection provides a reasonably accurate statistical model. Our strategy is thus to refit our model for water filling to simulations of the practical loading algorithm of [15]. We again propose a log-normal distribution for δ , which will be verified through simulations.

The mean value deviates from that of water filling since practical algorithms can only assign an integer number of bits per symbol and therefore suffer from a performance penalty, expressed as (15). The markers in Fig. 7 present simulation results for this penalty. We can store these values in a table and interpolate between them if necessary. Alternatively

$$\Delta\mu_{\delta(\text{decibel})} = \mu_{\delta(\text{decibel})}^{\text{water filling}} - \mu_{\delta(\text{decibel})}^{\text{loading}} \quad (15)$$

$$\Delta\mu_{\delta(\text{decibel})} \approx 0.342(1 + 2^{-0.9b_{\text{av}}+0.5}) \times (1 + 2^{-0.022 \cdot N - 4.4}) \quad (16)$$

provides a close approximation, as indicated by the solid lines in Fig. 7.

From numerous simulations, which we do not include here due to space limitations, we have learned that the variance in the case of practical bit-loading algorithms is the same as

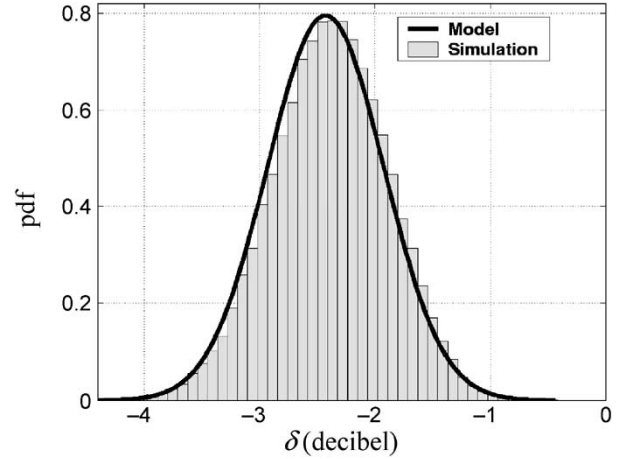


Fig. 8. Simulated results and model for the pdf of δ for bit loading and uncorrelated fading.

that for water filling. Our stochastic model for adaptive loading therefore consists of the following elements.

- 1) The distribution of δ is log-normal.
- 2) The mean value of δ (in decibels) is given by (12) and (13), augmented with (16).
- 3) The variance of δ (in decibels) is given by (14).

To validate this model, we compare it to a simulated histogram, as shown in Fig. 8 for $N = 100$ and $b_{\text{av}} = 4$ bits/symbol. Note that these values are different from the ones we used when deriving our model, where N was equal to 32, 128, 512, or 2048. We repeated these simulations for the other values of (N, b_{av}) tuples, resulting in similar fits. Note, however, that strictly speaking our results only apply to the algorithms described in [10]–[12] and [15]. We expect that very similar expressions can be found for other practical bit-loading algorithms as well. This probably only requires adjusting (16), as both the basic distribution and the variance appear to be primarily determined by averaging over the N subcarriers, which is essentially present in all algorithms.

V. PDF OF δ FOR CORRELATED FADING

The probabilistic model we described in the previous subsection is valid when the fading on the subcarriers is uncorrelated in frequency. In this section, we develop a model for correlated fading, where the channel gains on adjacent carriers are mutually correlated. As in the uncorrelated case, the time dependencies are determined by the Doppler rate, as explained in Section III.

The correlation between the subcarriers is characterized by the coherence bandwidth of the channel f_{coh} , which gives the frequency spacing where the correlation coefficient drops below 1/2 [8]. As such, it is a measure for the size of the frequency range over which subcarriers are more or less correlated. The equivalent number of independent subcarriers, which we denote by parameter M , is thus approximately equal to the total frequency band occupied by the multicarrier system, divided by the coherence bandwidth. Since f_{coh} is roughly inversely proportional to the root mean square delay spread

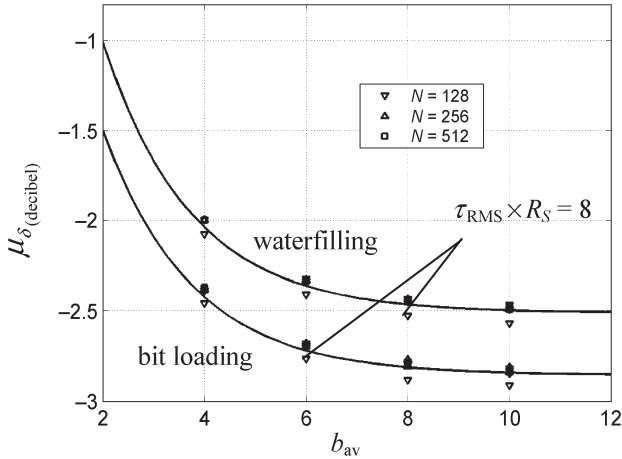


Fig. 9. μ_{δ} (decibel) versus b_{av} for correlated fading.

of the channel τ_{RMS} [8] and the total frequency band is proportional to the OFDM channel symbol rate R_S , M exhibits the trend

$$M \propto \frac{R_S}{f_{coh}} \propto \tau_{RMS} R_S. \quad (17)$$

For a fixed delay spread, M is independent of N , as only the number of carriers in the correlation bandwidth increases, and more are correlated as N increases. Equation (17) gives the general trend and is not to be interpreted as an exact relationship. The reason is that the delay spread and the coherence bandwidth are defined rather arbitrarily, and as such are not directly related to the “equivalent number of uncorrelated subcarriers” [8]. However, (17) provides a good starting point for our model in the case of correlated fading between subcarriers.

In the case of uncorrelated fading, the distribution of δ was log-normal, for both water filling and bit loading, because of the independent contributions from all subcarriers, as detailed in Appendix B. The same is expected to hold true here, except that there are now only about M independent contributions. If M is not too small, we therefore expect again a log-normal distribution, which we will verify later on through simulations.

Fig. 9 plots the mean value for both water filling and bit loading in the case of correlated fading. The markers denote simulated values for different N and $\tau_{RMS} R_S = 8, 16, 32$, and 64 . The solid lines correspond to the same model as for uncorrelated fading, given by (12), (13), and (16). This model is again reasonably accurate, except for the small deviation for $N = 128$ and $\tau_{RMS} R_S = 8$. In this case, there are few subcarriers of which very few are independent, and the stationarity assumption of Appendix B starts to break down here.

Following the same reasoning as above, the equations for the variance are expected to be very similar as before, namely given by (14), except that N is replaced by M . Unlike the mean value and the basic shape of the distribution, where M just needed to be large enough, the variance is much more sensitive to the exact expression of M . From simulations, we have derived that replacing N in (14) by M provides good results if θ is set to 2 and M is given by

$$M = 3.85[\tau_{RMS} \times R_S]^{0.9}. \quad (18)$$

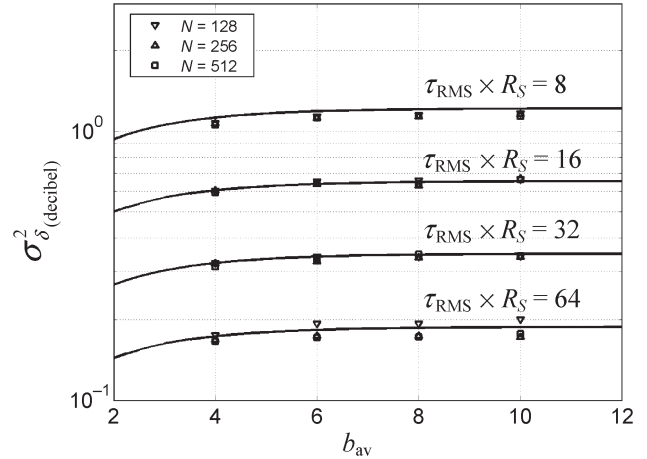


Fig. 10. σ_{δ}^2 (decibel) versus b_{av} for correlated fading.

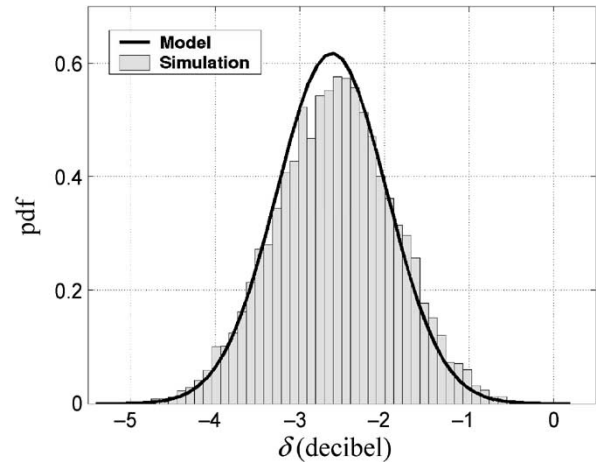


Fig. 11. Simulated results and model for the pdf of δ for bit loading and correlated fading.

As mentioned earlier, (17) only indicated a general trend for M . Fig. 10 compares the simulated values, denoted by markers, to the expressions we propose here. The results are shown for practical bit loading, but they are the same for water filling.

Given the expressions for the mean value and variance that we proposed above, we now validate our entire model for correlated fading. In Fig. 11, the resulting pdf of δ (in decibels) is compared to a simulated histogram. As an example, we choose $N = 512$, $b_{av} = 5$ bits/symbol and $\tau_{RMS} \times R_S = 20$. Although the fit is not as perfect as for uncorrelated fading, it is still accurate enough in practice, as we show in the next section.

VI. EXAMPLE: PACKET LENGTH ADAPTATION

Here, we illustrate how the model we presented in the previous sections can be used when simulating systems that have loaded multicarrier modulation as a physical layer. Our model is useful for any protocol of the OSI stack that depends on bit-level error statistics. As an example, we consider here a system that performs packet length adaptation [4] and simulate its performance.

To transmit data, bits are grouped into packets. Such packets not only carry data (L bits) but also require a packet header

(H bits). We assume this header contains a cyclic redundancy check (CRC) to determine when the packet contains errors caused by transmission over the wireless channel. The packet error rate (PER) is related to the BER by (19). For practical values of the BER, this expression can be very closely approximated as (20).

$$\text{PER} = 1 - (1 - \text{BER})^{L+H} \quad (19)$$

$$\text{PER} \approx (L + H)\text{BER}. \quad (20)$$

A key performance metric is called the “goodput,” which is the number of useful data bits that are transmitted successfully [4]. It takes into account the fact that the header overhead and erroneous transmissions do not contribute useful data, and is given by [4]

$$G = \left(\frac{R_s \times b_{\text{av}}}{L + H} \right) (1 - \text{PER})L. \quad (21)$$

It has been recognized that operating with a fixed packet size over an inherently variable wireless channel is inefficient in terms of goodput [4]. Instead, the packet size can be adapted based on the momentary channel condition, characterized by the BER. We calculate the optimal packet size by combining (20) and (21) and taking the derivative for L , resulting in

$$L_{\text{opt}} = H \left(\frac{1}{\sqrt{H \cdot \text{BER}}} - 1 \right). \quad (22)$$

The system periodically estimates the BER by averaging the measured bit errors over a fixed time window and then chooses the packet length based on (22). Fig. 12 illustrates how our model can be used to simulate packet length adaptation. We choose $H = 32$ bits, $N = 512$, $b_{\text{av}} = 5$ bits/symbol, and $\tau_{\text{RMS}} \times R_s = 20$. On one hand, we generate a large set of channels, perform loading on them, and calculate the BER estimate based on (7) and (11). This estimate together with (22) sets the packet size, and we evaluate the goodput via bit true simulations (shown in Fig. 12 as “bit true”). On the other hand, we pick δ values from the distribution generated by our model, plug them into (7), and evaluate (21) with L given by (22). Fig. 12 shows the cumulative distribution of G for both cases. As a basis of comparison, the system performance with a fixed packet size is also plotted, illustrating the benefits of packet length adaptation even in loaded multicarrier systems. We conclude that picking δ from the distribution indeed gives us the same results as the ones we would have obtained through a full-bit true simulation of the adaptive loading. As such, this validates the model we proposed in Section V.

The packet length adaptation we discussed is just one example of a large set of research problems where our statistical model can be beneficial. When designing a system that is affected by channel variability and possibly adapts accordingly, simulations that incorporate an accurate yet fast description of this channel behavior are an essential aid. Besides other link layer techniques, such research includes wireless packet scheduling, transmission control protocol (TCP) over wireless links, and channel-aware routing schemes, among others. In

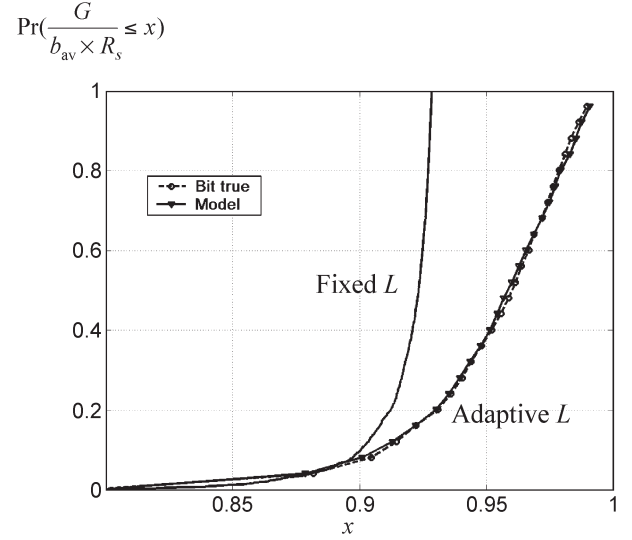


Fig. 12. Cumulative distribution of the normalized G .

addition, the statistical description provided by our model also offers the possibility to calculate mathematical performance characteristics such as the outage probability for example.

VII. CONCLUSION

When channel variations are slow enough such that they can be tracked efficiently, adaptive loading greatly improves the performance of multicarrier systems. First, we have proven that, from a performance point of view, a loaded multicarrier system can be regarded as a single carrier one with a single flat-fading channel tap. As a result, protocols such as packet length adaptation that were designed to combat channel variations in single carrier systems are thus applicable here as well, provided that the statistics are modified accordingly. Second, we have presented equations that predict the distribution of this single parameter for both uncorrelated and correlated fading. This allows us to model a loaded multicarrier system very efficiently for simulation purposes, resulting in significant speed-ups during protocol and system evaluation and development. Third, our model offers the necessary statistics for mathematical performance analysis. As an example, we have the benefits of our approach in a system that adapts the frame length in response to performance variability in the physical layer.

APPENDIX A

DERIVING THE SINGLE PARAMETER DESCRIPTION

In this Appendix, we derive the single parameter equivalent model of the loaded multicarrier system through a systematic analysis. The average transmit power P_{av} , defined in (9), can be rewritten as

$$P_{\text{av}} = \frac{1}{N} \frac{P_n}{A} \sum_{i=1}^{\tilde{N}} \frac{\text{SNR}_i}{\alpha_i} \quad (\text{A1})$$

by using (2).

By combining this expression with (4), we get (A2). Since all loading algorithms satisfy (6), this can in turn be rewritten as (A3)

$$P_{\text{av}} = \frac{1}{N} \frac{P_n}{A} \sum_{i=1}^{\tilde{N}} \frac{\Gamma_i}{\alpha_i} (2^{b_i} - 1) \quad (\text{A2})$$

$$P_{\text{av}} = \frac{P_n \Gamma}{A} \frac{1}{N} \sum_{i=1}^{\tilde{N}} \frac{(2^{b_i} - 1)}{\alpha_i}. \quad (\text{A3})$$

We define a variable δ as (A5), such that we can simplify (A3) to (A4). Note that this new expression for the transmit power is solely the result of algebraic substitutions, without any approximations

$$P_{\text{av}} = \frac{P_n \Gamma}{A} \frac{(2^{b_{\text{av}}} - 1)}{\delta} \quad (\text{A4})$$

$$\delta = \frac{2^{b_{\text{av}}} - 1}{\frac{1}{N} \sum_{i=1}^{\tilde{N}} \frac{2^{b_i} - 1}{\alpha_i}}. \quad (\text{A5})$$

By reordering (A4) and substituting Γ back from (5) without the subindex, we obtain

$$\text{BER} = \frac{K}{b_{\text{av}}} Q \left(\sqrt{3 \frac{\delta}{2^{b_{\text{av}}} - 1} \frac{P_{\text{av}}}{P_n} A} \right). \quad (\text{A6})$$

Although it is possible to calculate parameter K exactly, it is well recognized that the impact of K in expressions like (A6) is minor [8]. We propose to approximate K as

$$K = 4 \left(1 - \frac{1}{2^{\frac{b_{\text{av}}}{2}}} \right) \quad (\text{A7})$$

in analogy with (3) to simplify the calculations.

Equation (A6) suggests that the BER is uniform, which is not exactly true. Since only the gap is the same for the various subcarriers, BER_i is not exactly equal. Nevertheless, the differences are small and virtually insignificant at the system operating points of interest. As a result, the overall BER, given by (A6), can typically be considered as being uniform for practical purposes. The example of packet length adaptation, discussed in Section VI, illustrates this fact as well.

APPENDIX B

DERIVING THE PDF OF δ FOR UNCORRELATED FADING

Water filling assigns the power and bits to the subcarriers according to

$$P_i = \begin{cases} \varepsilon - \frac{\Gamma P_n}{\alpha_i A}, & \text{when } \alpha_i > \frac{\Gamma P_n}{\varepsilon A} \\ 0, & \text{otherwise} \end{cases} \quad (\text{B1})$$

$$b_i = \log_2 \left(\frac{\alpha_i \varepsilon A}{\Gamma P_n} \right), \quad \text{when } P_i > 0. \quad (\text{B2})$$

The parameter ε (a Lagrange multiplier in the derivation of these expressions [16]) links the two equations. For each of the loaded subcarriers, (B2) gives the assigned constellation. The value of ε is increased until the data rate constraint is satisfied [i.e., the required b_{av} is reached, defined as (10)]. From (B1), it is clear that at the same time the total power budget increases more subcarriers are assigned a nonzero transmit power, i.e., more of them become loaded.

In (B3), we define a constant $\tilde{\alpha}$, which allows us to simplify (B2) as (B4). From this last equation, we can see that $\tilde{\alpha}$ physically corresponds to the threshold value of α_i for which b_i would be exactly equal to 0

$$\tilde{\alpha} \triangleq \frac{\Gamma P_n}{\varepsilon A} \quad (\text{B3})$$

$$b_i = \log_2 \left(\frac{\alpha_i}{\tilde{\alpha}} \right). \quad (\text{B4})$$

Consequently, we substitute (B4) in (10) for the average overall bit rate, resulting in (B5). Through algebraic substitution, this is simplified to (B6) and (B7)

$$b_{\text{av}} = \frac{1}{N} \sum_{i=1}^{\tilde{N}} \log_2 \left(\frac{\alpha_i}{\tilde{\alpha}} \right) \quad (\text{B5})$$

$$b_{\text{av}} = \frac{\tilde{N}}{N} \left[\log_2 \left(\frac{1}{\tilde{\alpha}} \right) - \Omega_{\tilde{N}} \right] \quad (\text{B6})$$

$$\Omega_{\tilde{N}} \triangleq \frac{1}{\tilde{N}} \sum_{i=1}^{\tilde{N}} \log_2 \left(\frac{1}{\alpha_i} \right). \quad (\text{B7})$$

At this point, we note that the definition of δ , given by (11), is valid irrespective of the loading algorithm and therefore also for water filling. Furthermore, we can modify this definition to (B8) by substituting b_i from (B4). This is further rewritten to (B9) and (B10)

$$\delta = \frac{2^{b_{\text{av}}} - 1}{\frac{1}{N} \sum_{i=1}^{\tilde{N}} \left(\frac{1}{\tilde{\alpha}} - \frac{1}{\alpha_i} \right)} \quad (\text{B8})$$

$$\delta = \frac{2^{b_{\text{av}}} - 1}{\frac{\tilde{N}}{N} \left(\frac{1}{\tilde{\alpha}} - \Delta_{\tilde{N}} \right)} \quad (\text{B9})$$

$$\Delta_{\tilde{N}} \triangleq \frac{1}{\tilde{N}} \sum_{i=1}^{\tilde{N}} \frac{1}{\alpha_i}. \quad (\text{B10})$$

By solving $\tilde{\alpha}$ from (B6) and substituting it in (B9), we get (B11) for δ , which only depends on b_{av} and the channel gains α_i

$$\delta = \frac{N}{\tilde{N}} \left[\frac{2^{b_{\text{av}}} - 1}{2^{b_{\text{av}} \frac{N}{\tilde{N}} + \Omega_{\tilde{N}}} - \Delta_{\tilde{N}}} \right]. \quad (\text{B11})$$

Unlike (11), which is valid for any loading algorithm, (B11) does not explicitly contain the values of b_i . This equation only applies to water filling. In theory, the statistics of δ can be derived from (B11) provided the statistics of α_i are known. We use the notation $f_\alpha(\alpha)$ to represent the pdf of these channel gains.

However, deriving the exact statistics is hard. Instead, we gradually construct our model by building it on top of solutions for simplified constraints. First, consider water filling when the bit rate requirement b_{av} increases to very large values. Since this means that the individual b_i have to increase as well, (B2) tells us that threshold ε has to go up and ever fewer subcarriers remain unloaded. As a result, for b_{av} going to infinity, \tilde{N} tends to N . This allows us to rewrite (B11) as (B12). Since $b_{\text{av}} \rightarrow \infty$, this can be further simplified to (B13)

$$\log_2(\delta) = \log_2(2^{b_{\text{av}}} - 1) - \log_2(2^{b_{\text{av}} + \Omega_N} - \Delta_N) \quad (\text{B12})$$

$$\log_2(\delta) = -\Omega_N = \frac{1}{N} \sum_{i=1}^N \log_2(\alpha_i). \quad (\text{B13})$$

In this case, $\log_2(\delta)$ is the sum of independent contributions. As a consequence, the central limit theorem states that for not too small values of N , the pdf approaches a Gaussian distribution [8, pp. 58–59]. Equivalently, δ is approximately log-normally distributed. It therefore suffices to determine the mean and variance of $\log_2(\delta)$ to describe the entire distribution. Upon close investigation of the general equation (B11) for water filling, we observe that the channel statistics only appear in averaged form. As a reasonable approximation, we propose therefore that for finite values of b_{av} , δ is log-normally distributed (for not too low N) as well. In Section IV-A, we verify this statement through simulations.

For calculating the variance, we again start from the special case where b_{av} goes to infinity. From (B13), we immediately derive the corresponding expression

$$\sigma_{\log_2(\delta)}^2 = \frac{\sigma_{\log_2(\alpha_i)}^2}{N} \quad (\text{B14})$$

for the variance of $\log_2(\delta)$ [8].

In practice, when b_{av} is not very large, a certain fraction of subcarriers remain often unused, such that \tilde{N} is actually smaller than N and the results for $b_{\text{av}} \rightarrow \infty$ are no longer valid. Nevertheless, we try to augment these results for arbitrary values of b_{av} . We postulate that the variance remains inversely proportional to N and that the proportionality factor is only a function of b_{av} . To obtain this proportionality factor, we have curve fitted the simulation data of Fig. 5, which resulted in (14) for the variance.

In order to calculate an expression for the mean value of the distribution, we first investigate the situation where N tends towards infinity. In this case, all probabilistic elements disappear from (B11) and the pdf of δ becomes a Dirac impulse. Prior work regarding the average capacity of fading channels essentially reports on the performance in case of an infinite N [5]–[7]. When N goes to infinity, (B6) and (B8)

give rise in the coupled integral equations (12) and (13). When the number of subcarriers is finite, as is the case in practical systems, δ corresponds to a distribution. If the process would be stationary in N , the result for N going to infinity would give us the expected value we are looking for. Luckily, simulations show that assuming stationarity for a not too small N is a reasonable approximation of the true process such that we propose to use (12) and (13) to calculate the mean value.

REFERENCES

- [1] J. Bingham, "Multicarrier modulation for data transmission: An idea whose time has come," *IEEE Commun. Mag.*, vol. 28, no. 5, pp. 5–14, May 1990.
- [2] *Wireless LAN Medium Access Control (MAC) and Physical Layer (PHY) Specifications*, Supplement to IEEE Standard for Information Technology, IEEE Standard 802.11a-1999.
- [3] L. Van der Perre, S. Thoen, P. Vandenameele, B. Gyselinck, and M. Engels, "Adaptive loading strategy for a high speed OFDM-based WLAN," in *Proc. IEEE Global Telecommunications (GLOBECOM)*, Sydney, Australia, 1998, pp. 1936–1940.
- [4] P. Lettieri, C. Schurgers, and M. B. Srivastava, "Adaptive link layer strategies for energy efficient wireless networking," *Wireless Netw.*, vol. 5, no. 5, pp. 339–355, 1999.
- [5] A. Goldsmith and P. Varaiya, "Capacity of fading channels with channel side information," *IEEE Trans. Inf. Theory*, vol. 43, no. 6, pp. 1986–1992, Nov. 1997.
- [6] M.-S. Alouini and A. Goldsmith, "Capacity of Rayleigh fading channels under different adaptive transmission and diversity-combining techniques," *IEEE Trans. Veh. Technol.*, vol. 48, no. 4, pp. 1165–1181, Jul. 1999.
- [7] L. Goldfeld and V. Lyandres, "Capacity of the multicarrier channel with frequency selective Nakagami fading," *IEICE Trans. Commun.*, vol. E83-B, no. 3, pp. 697–702, Mar. 2000.
- [8] J. Proakis, *Digital Communications*, 3rd ed., ser. Electrical and Computer Engineering. New York: McGraw-Hill, 1995.
- [9] A. Leke and J. Cioffi, "A maximum rate loading algorithm for discrete multicarrier modulation systems," in *IEEE Global Telecommunications (GLOBECOM)*, Phoenix, AZ, 1997, pp. 1514–1518.
- [10] D. Hughes-Hartogs, "Ensemble modem structure for imperfect transmission media," U.S. Patent 4 679 227, Jul. 7, 1987.
- [11] —, "Ensemble modem structure for imperfect transmission media," U.S. Patent 4 731 816, Mar. 15, 1988.
- [12] —, "Ensemble modem structure for imperfect transmission media," U.S. Patent 4 833 796, May 30, 1989.
- [13] P. Chow, J. Cioffi, and J. Bingham, "A practical discrete multitone transceiver loading algorithm for data transmission over spectrally shaped channels," *IEEE Trans. Commun.*, vol. 43, no. 2/3/4, pp. 773–775, Feb./Mar./Apr. 1995.
- [14] R. Fischer and J. Huber, "A new loading algorithm for discrete multicarrier transmission," in *Proc. IEEE Global Telecommunications (GLOBECOM)*, London, U.K., Nov. 1996, pp. 724–728.
- [15] S. Lai, R. Cheng, K. Letaief, and R. Murch, "Adaptive Trellis coded MQAM and power optimization for OFDM transmission," in *Proc. IEEE Vehicular Technology Conf. (VTC)*, Houston, TX, 1999, pp. 290–294.
- [16] I. Kalet, "The multitone channel," *IEEE Trans. Commun.*, vol. 37, no. 2, pp. 119–124, Feb. 1989.
- [17] C. Wong, R. Cheng, K. Lataief, and R. Murch, "Multiuser OFDM with adaptive subcarrier, bit, and power allocation," *IEEE J. Sel. Areas Commun.*, vol. 17, no. 10, pp. 1747–1758, Oct. 1999.
- [18] W. Rhee and J. Cioffi, "Increase in capacity of multiuser OFDM system using dynamic subchannel allocation," in *Proc. IEEE Vehicular Technology Conf. (VTC Spring)*, Tokyo, Japan, May 2000, pp. 1085–1089.
- [19] C. Yih and E. Geraniotis, "Adaptive modulation, power allocation and control for OFDM wireless networks," in *Proc. IEEE Personal, Indoor and Mobile Radio Communications (PIMRC)*, London, U.K., Sep. 2000, pp. 809–813.
- [20] ETSI, "HYPERLAN type 2 technical specification physical layer," Tech. Rep. ETSI TS 101 475 V1.12.A1, Jun. 2000.
- [21] S. Thoen, L. Van der Perre, B. Gyselinckx, M. Engels, and H. De Man, "Predictive adaptive loading for HIPERLAN II," in *Proc. IEEE Vehicular Technology Conf. (VTC Fall)*, Boston, MA, Sep. 2000, pp. 2166–2172.

- [22] Flarion Technologies. [Online]. Available: <http://www.flarion.com/>
- [23] CISCO Systems. [Online]. Available: <http://www.cisco.com>
- [24] A. Mood, G. Garybill, and D. Boes, *Introduction to the Theory of Statistics*. New York: McGraw-Hill, 1985.
- [25] S. Thoen, L. Van der Perre, M. Engeles, and H. De Man, "Adaptive loading for OFDM/SDMA-based wireless networks," *IEEE Trans. Commun.*, vol. 50, no. 11, pp. 1798–1810, Nov. 2002.
- [26] B. Canpolat and Y. Tanik, "Performance analysis of adaptive loading OFDM under Rayleigh fading," *IEEE Trans. Veh. Technol.*, vol. 53, no. 4, pp. 1105–1115, Jul. 2004.



Curt Schurgers (M'03) received the M.S.E.E. degree from the Katholieke Universiteit Leuven (KUL), Belgium, in 1997, and the Ph.D. degree from the University of California at Los Angeles, in 2002.

In 2003, he was a Postdoctoral Researcher at the Massachusetts Institute of Technology, Cambridge. He is now an Assistant Professor in the Electrical and Computer Engineering Department at the University of California, San Diego. His current research interests are wireless networks, low power systems, and sensor networks.



Mani B. Srivastava (S'87–M'90–SM'02) received the Ph.D. degree in electrical engineering and computer science from the University of California at Berkeley in 1992.

Prior to joining the University of California at Los Angeles (UCLA) in 1996, for five years he was a Member of the Networked Computing Research Department at Bell Laboratories, Murray Hill, NJ. He is currently a Professor with the Electrical Engineering Faculty of UCLA, where he directs the Networked and Embedded Systems Laboratory (<http://nesl.ee.ucla.edu>). He is also associated with the UCLA Center for Embedded Networked Sensing (CENS), a National Science Foundation (NSF) Science and Technology Center. He co-leads the Systems Area Research at CENS and is also a Deputy Director of the Center. His current interests are in embedded sensor and actuator networks, wireless and mobile systems, embedded system, power-aware computing and communications, and ubiquitous computing.

Dr. Srivastava currently serves on the Editorial Boards of the IEEE TRANSACTIONS ON MOBILE COMPUTING and the ACM Transactions on Sensor Networking, and has been Program Co-chair for ACM MobiHoc '03, ACM SenSys '03, and IEEE/ACM IPSN '05. He was the recipient of the NSF CAREER Award, the Okawa Foundation Grant, and the President of India's Gold Medal.